



**HAL**  
open science

## Detection of variance changes and mean value jumps in measurement noise for multipath mitigation in urban navigation

Mariana Spangenberg, Jean-Yves Tourneret, Vincent Calmettes, Grégoire Duchâteau

► **To cite this version:**

Mariana Spangenberg, Jean-Yves Tourneret, Vincent Calmettes, Grégoire Duchâteau. Detection of variance changes and mean value jumps in measurement noise for multipath mitigation in urban navigation. Asilomar 2008, 42nd Conference on Signals Systems and Computers, Oct 2008, Pacific Grove, United States. pp 1193-1197, 10.1109/ACSSC.2008.5074604 . hal-01022442

**HAL Id: hal-01022442**

**<https://enac.hal.science/hal-01022442>**

Submitted on 30 Sep 2014

**HAL** is a multi-disciplinary open access archive for the deposit and dissemination of scientific research documents, whether they are published or not. The documents may come from teaching and research institutions in France or abroad, or from public or private research centers.

L'archive ouverte pluridisciplinaire **HAL**, est destinée au dépôt et à la diffusion de documents scientifiques de niveau recherche, publiés ou non, émanant des établissements d'enseignement et de recherche français ou étrangers, des laboratoires publics ou privés.

# DETECTION OF VARIANCE CHANGES AND MEAN VALUE JUMPS IN MEASUREMENT NOISE FOR MULTIPATH MITIGATION IN URBAN NAVIGATION

*M. Spangenberg*<sup>(1)(2)</sup>, *J.-Y. Tourneret*<sup>(1)(3)</sup>, *V. Calmettes*<sup>(1)(4)</sup> and *G. Duchâteau*<sup>(2)</sup>

<sup>(1)</sup>TéSA laboratory, 14-16 Port Saint Etienne, 31000 Toulouse, France

<sup>(2)</sup>Thales Alenia Space - 26 ave J. F. Champollion, 31037 Toulouse cedex, France

<sup>(3)</sup>University of Toulouse/ENSEEIH/IRIT - 2 rue Charles Camichel, BP 7122, 31071 Toulouse cedex 7, France

<sup>(4)</sup>University of Toulouse/ISAE - 10 av. Edouard Belin, 31055 Toulouse Cedex 4, France

email: mariana.spangenberg@tesa.prd.fr, jean-yves.tourneret@enseeiht.fr, vincent.calmettes@isae.fr

## ABSTRACT

**This paper studies an urban navigation filter for land vehicles. Typical urban-canyon phenomena as multipath and GPS outages seriously degrade positioning performance. To deal with these scenarios a hybrid navigation system using GPS and dead-reckoning sensors is presented. This navigation system is complemented by a two-step detection procedure that classifies outliers according to their associated source of error. Two different situations will be considered in the presence of multipath. These situations correspond to the presence or absence of line of sight for the different GPS satellites. Therefore, two kinds of errors are potentially “corrupting” the pseudo-ranges, modeled as variance changes or mean value jumps in noise measurements. An original multiple model approach is proposed to detect, identify and correct these errors and provide a final consistent solution.**

## 1. INTRODUCTION

Personal land navigation is becoming one of the most widely spread global navigation satellite system (GNSS) application. In particular, vehicle navigation is nowadays part of many people’s daily life. New navigation-based services are demanding higher precision solutions. Different types of obstacles such as high buildings, trees or tunnels, create an important degradation in the precision of the estimated position. In urban canyon scenarios two main problems are to be considered: a partial or total outage in the satellite visibility, and the lack of integrity in the received pseudo-range measurement. Several approaches to cope with these problems are proposed within the GNSS community. The first problem is commonly addressed by complementing the satellite based navigation system with a dead-reckoning approach [1]. The principle is to use advantageously the redundancy of measurements. The second and most challenging problem is mainly caused by the presence of multipath. This article considers the different kind of errors affecting the received navigation signal in the presence of multipath, to consequently take advantage of an accurate measurement model.

Most commercial receivers address the multipath mitigation problem by performing an integrity check. This test is based on a receiver autonomous integrity monitoring (RAIM) strategy for detecting the “defective” signals [2]. However, this approach was conceived for aviation purposes under hypotheses that cannot be always applied to urban vehicle navigation. For instance, a minimum number of unbiased measurements are needed in order to do this integrity check. This condition cannot be ensured in urban canyon scenarios. Even in the very favorable case where these unbiased measurements were available, the noisy nature of the received signals would make this instantaneous integrity check to be highly inefficient. Within this context, this paper proposes a modified “integrity check” version adapted to urban areas.

Several methods can be found in the literature concerning multipath mitigation. Different configurations of antennas arrays are among the most typical hardware solutions [3]. Working on the receiver correlators to achieve code synchronization is another well known approach. However, determining the number of channels affected by multipath presents a major complexity [4]. In order to avoid these difficulties (and be hardware-independent), multipath correction can be performed on the final pseudo-range measurement. For instance, the contributions of all the multipath signals present at the receiver are summed up and the final error is modeled as a unique phenomenon. In this paper we propose to consider two different kinds of errors depending on the conditions in which the GPS signal is received.

Multipath signals can arrive to the receiver either in a line-of-sight (LOS) situation where the direct path is present (i.e. direct visibility over the corresponding satellite), either in a non-line-of-sight (NLOS) situation where the received signal contains multipath components only. In the first case, the errors introduced by multipath on the pseudo-range measurement depend on external time-varying parameters. These parameters include the density of the obstacle where the GPS signal was reflected, its distance from the moving vehicle, its relative phase with respect to the direct path signal, etc... This kind of multipath interference can be modeled by a noise variance jump in the received signal. For the NLOS case, (where just the reflected signal is tracked), the corrupted pseudo-range is affected by a mean value jump corresponding to a bias in the received signal [5, 6]. The main contribution of this paper is to study an appropriate algorithm for the detection of these two types of errors (LOS and NLOS) affecting the received GPS signal. It is important to note here that the final system will be based on a three hypothesis model: absence of error (nominal situation), presence of error and LOS, presence of error and NLOS.

Multipath detection has already received some attention in the literature. Giremus et al. [5] studied a Rao Blackwellized particle filter based on a jump Markov system. The proposed algorithm modeled the multipath NLOS situation by a mean value jump whose magnitude was jointly estimated with the vehicle position and velocity. Another two-hypothesis Bayesian approach was considered in [7]. The interfered signals were characterized by errors models based on Gaussian mixtures. However, the existing algorithms described above require to define a priori distributions for the NLOS error. This a priori knowledge is not easy to obtain in real urban scenarios. Moreover, the high computational cost of particle filters is a problem for land vehicle applications.

This paper studies a conventional extended Kalman filter (EKF) for the navigation solution. This filter is coupled with a two step approach for the detection and correction of errors affecting the received measurements. This approach is based on a hierarchical structure corresponding to a three hypothesis model. A first integrity check is performed to detect the presence of an anomaly in the corrupted signal using the EKF innovations. The second step consists of classifying the different sources of errors depending on

This work was supported by Thales Alenia Space.

the presence or absence of LOS. Errors observed in presence of LOS are modeled as variance changes. Conversely, errors observed in absence of LOS are modeled as mean value jumps as in [5, 6]. The detection of variance changes or mean value jumps is achieved using a scheme based on the Generalized Likelihood ratio (GLR) test. Finally, the parameters associated to the two kinds of errors (that have been detected in the first step) are jointly estimated and the measurement model is adapted considering the most likely error. Therefore, a correct characterization of the received signals will enable a more accurate solution for the estimated position.

The paper is organized as follows: Section 2 describes the navigation filtering models for urban scenarios. Different hypotheses about the conditions in which the signal is received are addressed here. The proposed algorithm for multipath interference mitigation is presented in section 3. Sections 3.3 and 3.4 provide a deeper analysis about the detection/identification/correction approach. Simulation results are presented in Section 4. Conclusions and perspectives are reported in Section 5.

## 2. NAVIGATION MODELS

The following state-space model is considered in this paper for the GPS navigation filter:

$$X_t = FX_{t-1} + w(t), \quad (1)$$

$$Y_t(t) = \sqrt{\|x_{s,t} - x_t\|^2} + b(t) + m_{i,t} + \sqrt{(\sigma_{i,t}^2 + r_{i,t}^2)}v_i(t), \quad (2)$$

where  $X_t$  is the state vector  $\in \mathbb{R}^8$  and  $Y_t$  is the measurement vector for  $i = 1, \dots, n_{sat}$ ,  $n_{sat}$  being the number of visible satellites. The state vector  $X_t$  is composed of the vehicle position  $x_t$  in the ECEF frame, its corresponding velocities and the receiver clock bias  $b_t$  and drift  $d_t$ . The state propagation matrix  $F$  in (1) corresponds to a random walk model where the acceleration has a Gaussian distribution. The state noise vector is represented by  $w(t)$ . The  $i$ th satellite position in the ECEF frame is denoted by  $x_{s,i}$ . The last term in (2) is the measurement noise whose nominal variance is denoted as  $\sigma_{i,t}^2$ , while  $v_i(t)$  is a zero mean Gaussian variable such that  $v_i(t) \sim \mathcal{N}(0, 1)$ . The two possible types of errors affecting the received measurement are denoted as  $m_{i,t}$  and  $r_{i,t}$  in (2). In nominal conditions, both  $m_{i,t}$  and  $r_{i,t}$  equal 0. In presence of LOS interference  $m_{i,t} = 0$  and  $r_{i,t}^2 \neq 0$ , whereas in NLOS situation  $m_{i,t} \neq 0$  and  $r_{i,t}^2 = 0$ . Thus,  $m_{i,t}$  characterizes the presence of a bias in absence of LOS whereas  $r_{i,t}^2$  defines the variance change associated to the presence of error in LOS.

## 3. MULTIPATH MITIGATION

### 3.1 Multi-hypothesis approach

Usual multipath mitigation schemes based on pseudo-range measurements consider a binary system where either the received signals are in LOS (i.e. bias-free), either they are in a NLOS situation (just the multipath signal is received) and a mean value jump is present. However, real scenarios are more complicated and a third option is possible corresponding to a composite signal due to the presence at the receiver antenna of a LOS and multipath signal. The error introduced by the multipath component will depend on its relative phase and delay with respect to the direct signal. Hence, this error will be continuously changing due to its dependence on not only the vehicle dynamics, but also on the local environment (the surfaces where the signal gets reflected). This paper models this error as a variance change in the additive noise. Although a change in the noise variance does not have such a strong impact on the positioning accuracy when compared to a mean value jump, it reveals to be a crucial factor when a precise bounding must be given for the final position solution.

A three hypothesis criterion is proposed to detect, identify and correct errors in the measurements:

- $H_0$ : absence of error (the received measurement is in LOS and not interfered), i.e.  $m_{i,t} = 0$  and  $r_{i,t}^2 = 0$ ,
- $H_1$ : the received measurement is in NLOS situation and affected by a mean value jump, i.e.  $m_{i,t} \neq 0$  and  $r_{i,t}^2 = 0$ ,
- $H_2$ : the received measurement is in LOS situation and is affected by a variance change in the additive noise, i.e.  $m_{i,t} = 0$  and  $r_{i,t}^2 \neq 0$ .

Under hypothesis  $H_0$ , the model error (i.e., the additive noise) has a Gaussian distribution. However, under hypotheses  $H_1$  and  $H_2$ , the nominal Gaussian distribution is no longer valid because of multipath presence. The errors associated to the two hypotheses  $H_1$  and  $H_2$  were modeled as a Gaussian mixture in [7]. However, when analyzed more in detail, this mixture model (obtained from a real navigation scenario) can be decomposed into a mean-shifted or a variance-increased Gaussian distribution (see figure 4 of [7]).<sup>1</sup>

### 3.2 System outline

The conditions in which signals are received in urban environments are constantly changing. The origin, magnitude and type of bias interfering the signals will depend on the satellite configuration and on the environment layout. Moreover, the error introduced by a multipath presence in an LOS situation, is different to the error introduced in an NLOS case. Hence, no a priori information about the evolution of the different multipath-based errors is assumed. To avoid imposing an error distribution, multipath presence is tested at every sampling period and its contribution to the measurement is estimated.

Due to the non linearity of the measurement model in (2) an EKF is used for the general navigation solution. A hierarchical method is proposed for error detection and later for error identification and quantification. The idea is that this multi-stage approach enables an urban-adapted navigation filter without entailing heavy computations in clear sky scenarios. The mitigation scheme is described as follows:

#### 1. Error detection

- The presence of an error is detected by performing an energy test on the innovations (this strategy is a direct result of the Neyman Pearson lemma).

#### 2. Error identification

- In case an error has been detected, a parallel processing is achieved for classifying the two possible sources of error. Two GLR tests are performed simultaneously for the detected outlier, since it can be affected by a mean value jump or by a variance change in the additive noise. The most likely hypothesis ( $H_1$  or  $H_2$ ) is considered for error correction.

#### 3. Error correction

- The received measurement model is updated either by a mean value jump or by a change in the noise variance, depending on the hypothesis that has been detected in the identification step. The corrected signal is then fed back to the main system (composed by the EKF) that computes the final position.

The proposed multi hypothesis approach can detect outliers, identify and correct different types of errors. The detection of measurement errors will be conducted by using the EKF innovations

$$I_i(t) = Y_i(t) - \hat{Y}_i(X_t), \quad (3)$$

as in [8], where  $\hat{Y}_i(X_t)$  is the measurement predicted from the propagated state vector. In nominal conditions, the innovations are dis-

<sup>1</sup>The actual mean value jump does not only represent an NLOS situation but also an LOS situation where the vehicle is not moving (i.e. the multipath delay and phase are constant, so its final contribution to the direct received signal is also a mean value jump). However, as this error is finally considered under the hypothesis  $H_1$ , the approach is still valid without loss of generality.

tributed according to a centered Gaussian distribution whose covariance matrix  $S_t$  is defined as follows:

$$S_t = H_t P_{t|t-1} H_t^T + R_t, \quad (4)$$

where  $H_t$  is the linearized measurement matrix and  $P_{t|t-1}$  is the a priori state covariance noise matrix. The innovations associated to different time instants are assumed to be independent. The variance of the  $i$ th innovation (denoted as  $s_{i,t}^2$ ) is given by the  $i$ th element of the diagonal of  $S_t$ . In this way, the  $i$ th innovation error is distributed according to a Gaussian distribution  $\mathcal{N}(0, s_{i,t}^2)$  under hypothesis  $H_0$  (i.e., in nominal situations).

The EKF minimizes the mean square error (MSE) of the state vector considering that the received measurements have a Gaussian distribution with known parameters. If such a hypothesis is not fulfilled, the convergence and stability of the filter are no longer guaranteed. Hence, a measurement subjected to any interference must be detected and its error distribution has to be characterized. Assuming the resultant distributions are Gaussian, the errors can be compensated and the EKF will still be able to provide a consistent solution. Details about the detection, estimation and correction of errors are provided in the following sections.

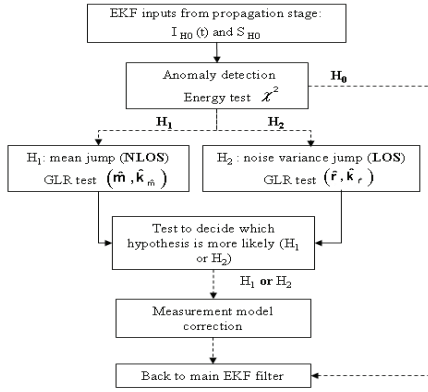


Figure 1: Filter scheme for the detection and correction of outliers.

### 3.3 Error detection

The first step of the algorithm detects the presence of corrupted signals referred to as outliers. The type of error affecting the signal is not specified at this point. A binary hypothesis test is performed to determine the absence (hypothesis  $H_0$ ) or presence (hypotheses  $H_1$  and  $H_2$ ) of an error in the measurements. The test is achieved for each of the received signals. A test based on the knowledge of the  $C/N_0$  ratio was presented in [7] to decide whether the received signal is error corrupted or not. However, if the multipath is in phase with the LOS signal, this test may no longer be valid. This paper considers a sliding window of  $N$  samples as observation window and assumes that the error (when it exists) is constant during this period of time. The energy of the innovations for each of the  $n_{\text{sat}}$  observation windows containing  $N$  samples is computed. The detection of errors is then achieved as follows:

$$T_{i,t} = \sum_{j=t-N+1}^t I_i^2(j) \stackrel{H_0}{\leq} \alpha_{i,t} \quad \forall i = 1, \dots, n_{\text{sat}} \quad (5)$$

where  $\alpha_{i,t}$  is the detection threshold related to the probability of false alarm (PFA) of the test. The test statistics  $T_{i,t}$  is distributed according to a central chi2 distribution with  $N$  degrees of freedom (denoted as  $\chi_N^2$ ), under hypothesis  $H_0$ . If the test statistics  $T_{i,t}$  exceeds the threshold  $\alpha_{i,t}$ , the presence of a error is declared and the error estimation procedure is used to determine the kind of error affecting the received signal.

Fig. 2 shows the error distributions under the hypotheses  $H_0$ ,  $H_1$  and  $H_2$ . It can be seen that the presence of error in the measurements (hypotheses  $H_1$  and  $H_2$ ) yields an innovation with larger energy than under hypothesis  $H_0$ . It is important to note that the threshold determination does not depend on the innovation distributions associated to  $H_1$  and  $H_2$ . Moreover, no knowledge about the mean value jumps and the variance changes in the additive noise have to be known to compute the test statistics.

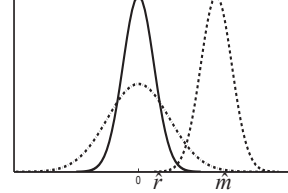


Figure 2: Error probability distribution for hypotheses  $H_0$  (solid line),  $H_1$  (dashed line) and  $H_2$  (dashed-dotted line).

The detected outlier is isolated from the solution in standard integrity checks, such as the RAIM algorithm. Such an approach is valid in clear sky scenarios where the received measurements are redundant. However, in urban environments, visibility over the GPS constellation is scarce and measurement exclusion may lead to an undetermined system. Therefore the maximum number of received measurements is needed to compute the position solution. Thus the detection step must be followed by the estimation and correction of the anomaly. This is the objective of the following sections.

### 3.4 Error identification and correction

As explained before, once an outlier has been detected, its source of error has to be identified and corrected. Estimates of  $m$  and  $r$  are computed and used to determine the final navigation solution. Due to the recursive nature of the EKF, not only the error magnitude must be estimated but also its time of occurrence. Note that the time of occurrence  $k$  of the error is generally smoothed within the observation window in (5), so that the effective time of detection does not match the real one. In case of missed detection, the error gets propagated through the state vector, and the estimated error magnitude can differ significantly from its real value. As a consequence, both hypotheses  $H_1$  and  $H_2$  depend on the error parameter  $m$  or  $r$  (that are supposed to be constant inside the observation window) and on the time of occurrence  $k$  (where  $k$  can take any value within the observation window  $t - N + 1 : t$ ) that should be estimated carefully. All expressions given hereafter will address just the detected outliers and should be applied to each of them.

The time occurrence estimation can be achieved by using the marginalized likelihood ratio (MLR) proposed by Gustafsson [9]. However, this test requires an a priori knowledge about the probability distributions of the parameters to be estimated (mean value jumps or variance changes in our case). A modified generalized likelihood ratio (GLR) is adopted in this paper [10] where each jump is considered as an unknown constant (as opposed to a random variable). The GLR proceeds for each detected outlier to a double maximization over the hypothesis variables  $v$  ( $v = m$  under hypothesis  $H_1$  and  $v = r$  under hypothesis  $H_2$ ) and  $k$  defined by

$$\hat{v}(k) = \arg \max_v l_i(k, v), \quad (6)$$

$$\hat{k} = \arg \max_k l_i(k, \hat{v}(k)), \quad (7)$$

$$l_i(k, v) = 2 \log \frac{p(Y_{t-N+1:t} | H_j(k, v))}{p(Y_{t-N+1:t} | H_0)}, \quad (8)$$

where  $j \in \{1, 2\}$ ,  $p(Y_{t-N+1:t} | H_j(k, v))$  represents the probability of observing an error at time instant  $k$  for  $Y_{t-N+1:t}$ , and  $l_i(k, v)$  is the log likelihood ratio. The method proposed in [10] is based on the idea that the relation between  $v$  and the EKF innovations can be

made explicit and represented as a linear regression. Then, after calculating the required regressors, a recursive least square bank of filters is implemented to find the values of  $\hat{v}(k)$ . However, even if a linear dependency for a mean value jump can be easily stated, this is not the case for variance changes. Therefore a suboptimal solution is considered in this paper. The error is calculated considering the  $N$  previous innovation samples as in [8]. More precisely, the mean value jump and the variance change are computed as

$$\hat{m}_t(k) = \frac{1}{t-k+1} \sum_{j=k}^t I(j), \quad (9)$$

$$\hat{r}_t^2(k) = \frac{1}{t-k+1} \sum_{j=k}^t \left\{ [I(j)]^2 - s_j^2 \right\}, \quad (10)$$

where the nominal innovation variance  $s_j^2$  (estimated under hypothesis  $H_0$ ) is subtracted from the calculated innovation variance in order to have the final variance jump. If this difference is negative, no variance jump is considered. An EKF is deployed to calculate for each  $k = t - N : t$  a likelihood ratio based on  $\hat{v}(k)$  associated to each detected outlier. Once the likelihood ratio exceeds an appropriate threshold  $\gamma$ , the corresponding  $\hat{k}$  is chosen as the candidate for the time of occurrence  $k$ :

$$\hat{k} = \min_k \{k; l_t(k, \hat{v}(k)) > \gamma\} \quad (11)$$

Once the threshold has been estimated, the error is assumed to be constant for the remaining samples of the sliding window. The filtering continues until time  $t$ , by taking into account the already detected error.

To conclude with the multi-hypothesis approach, a decision has to be taken regarding the kind of error that has been detected for each corrupted pseudo-range. Assuming both  $H_1$  and  $H_2$  have the same probabilities, the most likely hypothesis determines whether there is presence or absence of LOS in the received measurement  $Y^{t-N+1:t}$ . This is achieved using the following rule

$$p(Y_{t-N+1:t} | \hat{k}_{H_1}, \hat{m}_t(\hat{k}_{H_1})) \underset{H_2}{\overset{H_1}{\geq}} p(Y_{t-N+1:t} | \hat{k}_{H_2}, \hat{r}_t(\hat{k}_{H_2})) \quad (12)$$

with

$$p(Y_{t-N+1:t} | \hat{k}_{H_1}, \hat{m}_t(\hat{k}_{H_1})) \propto \sum_{j=t-N+1}^t \frac{[I_{H_1}(j)]^2}{s_j^2}, \quad (13)$$

$$p(Y_{t-N+1:t} | \hat{k}_{H_2}, \hat{r}_t(\hat{k}_{H_2})) \propto \sum_{j=t-N+1}^t \frac{[I_{H_2}(j)]^2}{s_j^2}, \quad (14)$$

where  $I_{H_1}^2(j)$  is the square of innovation corresponding to the  $j$ th time that has already been compensated by a mean value jump (i.e. considering  $H_1$ ). The innovation  $I_{H_2}^2(j)$  is analogous to  $I_{H_1}^2(j)$  but compensated by a change in the noise variance. Finally, the measurement model associated to every detected outlier has to be corrected and feedback to the update stage of the EKF algorithm. More precisely, a bias is removed from the innovations under hypothesis  $H_1$  whereas a variance is added to nominal variance under hypothesis  $H_2$ . These two corrections are summarized by the following relations

$$I(t)_{\text{corr}} = I(t) - \hat{m}_t, \quad (15)$$

$$\sigma_{t,\text{corr}}^2 = \sigma_t^2 + \hat{r}_t^2. \quad (16)$$

Note that the corrected variance  $\sigma_{t,\text{corr}}^2$  is used for the new computation of the measurement noise covariance matrix  $R$ . In this way, a final unbiased navigation solution is calculated.

## 4. SIMULATIONS

This section validates the proposed detection/estimation algorithm using simulated data. A vehicle trajectory has been generated according to the state model (1) with an acceleration variance of  $2m/s^2$ . The received pseudo-range measurements correspond to a simulated GPS constellation and have an associated noise standard deviation of  $\sigma = 12m$  in nominal conditions. The errors introduced in the measurements have been generated according to the model (2) as follows

- A mean value jump of  $40m$  is introduced in the satellite number 1, between the 30th and 60th second.
- A noise variance jump of  $40m$  affects the same satellite for a time interval of 40 seconds between the 100th and 140th second.
- A second satellite (satellite number 2) experiences a mean value jump of  $40m$  between the 110th and 150th second.

The simulated errors were introduced to highlight the performance of the proposed navigation filter. The first isolated mean value jump on satellite 1 (corresponding to hypothesis  $H_1$ ) is the type of error that more visibly affects the positioning accuracy. The correct functioning of the filter is tested for this critical situation. A simultaneous appearance of different errors is then studied. Two satellites are corrupted by different types of errors during overlapped time intervals. In this way, the algorithm is tested for its capacity to identify several defective measurements and their corresponding source of error. The threshold for the error detection in (5) has been adjusted in order to obtain  $FAP = 0.1\%$ . The observation window length is  $N = 5$  and the sampling period equals  $1Hz$ . The estimation of the error time of occurrence in (11) has been achieved with  $\gamma = 1$  (i.e. once the error presence has been detected, all time instants within the observation window are equally likely).

Figs 3 and 4 show the innovation pdfs corresponding to the two satellites corrupted by errors (satellites 1 and 2). The nominal gaussian pdf is depicted in red while the actual normalized pdf for the EKF innovations is shown in blue. The pdfs are obtained from all the available samples of the simulated satellites. The results are presented in Fig. 3(a) for a standard EKF (i.e. without any error control), and in Fig. 3(b) for the proposed enhanced detection/estimation filter. The innovations do not have a Gaussian distribution in the first case because the corrupted measurements are not compensated by the filter (the green circles highlight the *abnormal* components of the pdf). Conversely, when errors are corrected with the proposed algorithm, the histogram of the corrected innovations is close to the adjusted Gaussian pdf.

Fig. 5 presents similar results for the final estimated position. The absolute position errors (in 3D) are shown in blue and compared with their corresponding bounds illustrated in red. The bounds have been calculated from the updated EKF error covariance matrix  $P_t$ , i.e. using the following relation

$$B_t = 3\sqrt{\sigma_{x,t}^2 + \sigma_{y,t}^2 + \sigma_{z,t}^2}, \quad (17)$$

considering that all solutions should be included within 3 time the standard deviation. The non compensated contribution of the corrupted measurements is presented in Fig. 5(a). For this case, the final solution is either biased or not bounded during the intervals where errors are present. However, Fig. 5(b) shows that the position estimates are in good agreement with the bound thanks to the proposed detection/identification/correction scheme.

## 5. CONCLUSIONS

This paper presented an enhanced navigation system adapted to urban canyon scenarios. The innovation of the proposed approach relied on the way the received signals are processed: a two step procedure was used to detect *multiple* outliers and to classify these outliers according to the *different* types of errors affecting the navigation signal. A hierarchical three-hypothesis test was implemented. Two different situations were considered in the presence of multipath. These situations correspond to the presence or absence of line

of sight (referred to as LOS and NLOS situations) over the multiple GPS satellites. Therefore two kinds of errors were potentially “corrupting” the pseudo-ranges, modeled as noise variance or mean value jumps. A GLR detector was derived to determine the origin and quantify such errors. A multiple model EKF was considered as the best adapted solution for this fast-decision/on-line application. Simulation results presented for synthetic signals validated the relevance of the proposed algorithm.

Interesting future investigations include the application of the proposed scheme to different areas where similar problems may be encountered. For example, similar errors were considered to affect the mobile communication signals [6]. The proposed strategy should be interesting in this context.

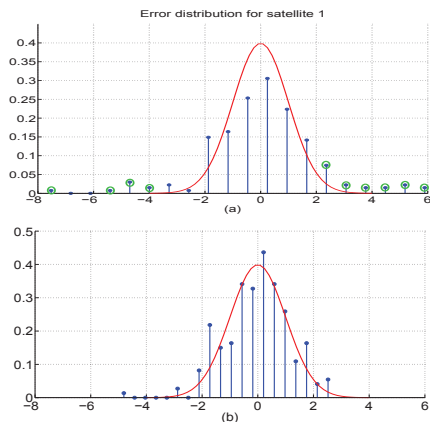


Figure 3: Innovation distributions for satellite 1 (a) Standard EKF and (b) Proposed detection/correction algorithm.

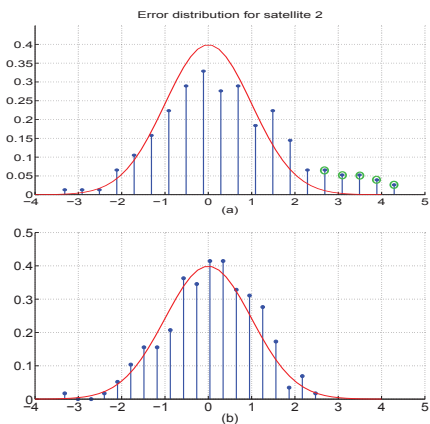


Figure 4: Innovation distributions for satellite 2. (a) Standard EKF and (b) Proposed detection/correction algorithm.

## REFERENCES

- [1] J. A. Farrell and M. Barth, *The Global Positioning System and Inertial Navigation*. New York: McGraw-Hill, 1999.
- [2] E. Kaplan and C. Hegarty, *Understanding GPS principles and applications*, ch. 7. Boston: Artech House, 2006.
- [3] M. Braasch, *Global Positioning System: theory and applications*, vol. 1, ch. 14. AIAA, 1996.
- [4] J. Soubielle, I. Fijalkow, P. Duvaut, and A. Bibaut, “GPS positioning in a multipath environment,” *IEEE Trans. Signal Process.*, vol. 50, no. 1, pp. 141–150, 2002.
- [5] A. Giremus and J.-Y. Tourneret, “Joint detection/estimation of multipath effects for the global positioning system,” in *Proc. ICASSP-05*, (Philadelphia, USA), May 2005.

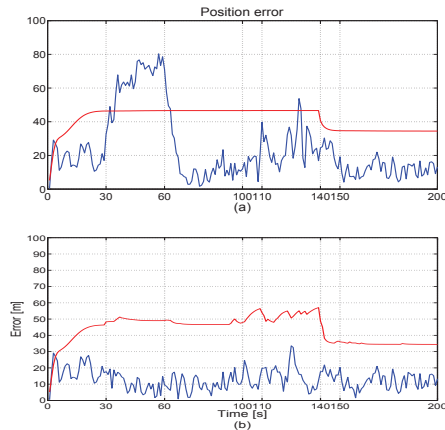


Figure 5: Final position errors and bounds (a) Standard EKF and (b) Proposed detection/correction algorithm.

- [6] J. Huerta and J. Vidal, “LOS-NLOS situation tracking for positioning systems,” in *Proc. SPAWC-06*, (Cannes, France), 2006.
- [7] N. Viandier, D. Nahimana, J. Marais, and E. Duflos, “GNSS performance enhancement in urban environment based on pseudo-range error model,” in *Position, Location and Navigation Symposium, 2008 IEEE/ION*, (Monterey, CA), May 2008.
- [8] C. Hajiyeve, “Innovation approach based measurement error self-correction in dynamic systems,” *Elsevier, Measurement Journal*, vol. 39, no. 7, pp. 585–593, 2006.
- [9] F. Gustafsson, *Adaptive filtering and change detection*, ch. 9. Wiley and Sons, 2000.
- [10] A. S. Willsky and H. Jones, “A generalized likelihood ratio approach to the detection and estimation of jumps in linear systems,” *IEEE Transactions on automatic control*, vol. 21, no. 1, pp. 108–112, 1976.